Malaysian Journal of Chemistry, 2024, Vol. 26(5), 431-441
(Special Issue: *4th IKMPB Online Symposium 2024 - Development of Chemistry to Accomplish a Sustainable World*)

Prednisolone-Loaded Solid Lipid Nanoparticles: Preformulation Studies and Physicochemical Characterisation

Aliya Nadira Mohd Zainudin[1], Aina Shahirah Mohd Shafri[1], Idanawati Naharudin[1,2], Meor Mohd Redzuan Meor Mohd Affandi[1] and Nor Khaizan Anuar[1,2,3]*

[1]Faculty of Pharmacy, Universiti Teknologi MARA, Cawangan Selangor, Kampus Puncak Alam, 42300 Bandar Puncak Alam, Selangor Darul Ehsan, Malaysia
[2]Non-Destructive Biomedical and Pharmaceutical Research Centre, Smart Manufacturing Research Institute, Universiti Teknologi MARA, 42300 Puncak Alam, Selangor, Malaysia
[3]Food Process and Engineering Research Group (FOPERG), Universiti Teknologi MARA, 40450 Shah Alam, Selangor Darul Ehsan, Malaysia
*Corresponding author (e-mail: norkhaizan2874@uitm.edu.my)

Prednisolone, a corticosteroid known for its anti-inflammatory and immunosuppressive properties, is administered either orally or via injection. The present research investigated the preformulation aspects and physicochemical characteristics of prednisolone-loaded solid lipid nanoparticles (SLNs), aiming to explore their potential as a transdermal drug delivery system. Prednisolone-loaded SLNs were prepared using the emulsification-ultrasonication technique, employing cetyl alcohol and Tween 20 as the solid lipid and surfactant, respectively. The Box-Behnken design assessed the impact of various independent variables, including lipid concentration, surfactant concentration, and lipid/drug ratio, on the measured particle size, polydispersity index (PDI), and zeta potential. Physicochemical characterisation was performed using attenuated total reflectance-Fourier transform infrared spectroscopy (ATR-FTIR) and transmission electron microscopy (TEM). The results demonstrated that the SLNs containing prednisolone had mostly rod-shaped or cuboidal particles, with an average size ranging from 59.99 to 594.70 nm. The PDI exhibited a range of values from 0.39 to 1, while the zeta potential was observed to vary between -34.37 and -15.73 mV. The ATR-FTIR analysis showed that the incorporation of prednisolone into the solid lipid of the nanoparticles was successful. This was confirmed by the masking of drug absorption peaks in the spectral range of 1600 to 3500 cm^{-1}, indicating that prednisolone was effectively loaded into the SLNs.

Keywords: Prednisolone; solid lipid nanoparticles; transdermal drug delivery; Box-Behnken design

Received: January 2024; Accepted: July 2024

The effectiveness of a treatment plan relies heavily on the adherence of patients to their prescribed medication regimen. However, adherence to steroid treatments can be challenging, particularly for individuals dealing with chronic conditions, due to various factors such as the need for consistent dosing, lengthy treatment durations, and potential side effects [1, 2]. Consequently, there is a growing prevalence of noncompliance with steroid therapy among this group of patients, leading to significant consequences, including increased medication wastage, disease progression, higher mortality rates, and elevated healthcare costs [3]. Prednisolone is a steroid used to reduce inflammation and suppress the immune response. The low molecular mass and moderate lipophilicity make it suitable for transdermal delivery. Administering prednisolone through transdermal delivery allows direct absorption into the systemic circulation. This decreases the first-pass effect of hepatic metabolism and eliminates the requirement for increased pre-metabolic doses when using oral prednisolone.

However, the skin's natural barrier function presents a challenge in transdermal drug delivery. It is essential to breach this protective barrier to improve the effectiveness of transdermal drug delivery. As a result, nanoparticles have been used as a method of advancement [4, 5]. Prior research has established that nanoparticles can transport drugs into the circulatory system over an extended duration, thus diminishing plasma fluctuations and averting adverse events [6, 7]. Solid lipid nanoparticles (SLNs) are drug delivery systems that can be utilised in various ways to improve drug bioavailability. SLNs are alternative carrier systems to standard colloidal carriers, such as emulsions, liposomes, and polymeric micro- and nanoparticles. Owing to their stability, biocompatibility, and low toxicity, lipid-based nanoparticles have received considerable attention as an effective drug delivery strategy [8].

It is widely recognised that the type and concentration of lipids and emulsifiers significantly

†Paper presented at the 4th IKMPB Online Symposium 2024 – Development of Chemistry to Accomplish a Sustainable World

influence the quality of SLN dispersion [9]. Response surface methodology (RSM) is a useful approach for analysing numerous process variables simultaneously when their interactions are intricate. RSM has proven to be effective in optimising various drug delivery systems [10, 11]. The current study employed the Box-Behnken design to develop and optimise prednisolone-loaded SLN formulations. This design is advantageous as it requires fewer experimental runs compared to other RSM designs and is particularly useful in avoiding extreme treatment combinations. Additionally, the polydispersity index, zeta potential, surface morphology, particle size, and chemical interactions of prednisolone-loaded SLN were examined.

EXPERIMENTAL

Chemicals and Materials

Prednisolone was purchased from Sigma-Aldrich (United States). Cetyl alcohol was obtained from Biotek Abadi (Malaysia), Tween 20 was supplied by Sigma-Aldrich (Germany), and absolute ethanol was purchased from Merck (Germany).

Characterisation Methods

Lipids Screening

Lipid screening was performed to determine the solid lipid with maximum drug solubility, ensuring optimal drug loading in the nanoparticles. Three candidate lipids, cetyl alcohol, cetostearyl alcohol, and cetyl palmitate, were evaluated for their ability to dissolve prednisolone. To assess the solubility, prednisolone and each lipid were physically mixed in test tubes at predetermined mass ratios of 99:1 and 95:5 (lipid:drug). Upon heating to achieve lipid melting, the mixtures were visually examined to determine the presence or absence of undissolved drug crystals. The lipid that showed the highest degree of prednisolone solubility was then utilised to develop prednisolone-loaded SLNs in subsequent trials.

Preparation of Prednisolone-loaded SLN

Prednisolone-loaded SLNs were prepared based on established protocols, with few modifications [9,12]. Briefly, cetyl alcohol (5% w/w) was melted above its melting point (60 ˚C). Prednisolone (1% w/w) was dissolved in 2 mL of ethanol, heated to 60 ˚C, and combined with a preheated (60 ˚C) mixture of Tween 20 (5% v/v) and distilled water (44.98 mL). The aqueous and lipid phases were combined and retained at 60 ˚C for 15 min with continuous stirring. Then, the warm emulsion was subjected to sonication using a Soniclean Digital Benchtop Ultrasonic bath at 100 W and 40 ˚C for 3 min with a 2-minute rest interval, forming prednisolone-loaded SLNs. This procedure was repeated for all formulations generated using Design-Expert software (Table 1).

Preformulation Optimisation using Box-Behnken Design

The Box-Behnken design, 17-run RSM approach, and a 3-factor, 3-level, were employed for model generation and optimisation. This design, implemented through Design-Expert software (Version 7, Stat-Ease Inc., MN), efficiently explored the quadratic response surface with minimal experimental runs in the presence of three variables. The region of interest is determined by replicated centre points and edge points, allowing for the assessment of the main effects, interaction effects, and quadratic impacts of formulation ingredients on the dependent variables. This design produces the subsequent nonlinear quadratic model.

$$Y = A_0 + A_1A + A_2B + A_3C + A_4AB + A_5BC + A_6AC + A_7A^2 + A_8B^2 + A_9C^2$$

Where Y represents the measured response of dependent variables for each combination of factor levels. The regression coefficients A_0 to A_9 are calculated from experimental data [13], and A, B, and C represent the independent variables coded as follows: A = lipid concentration, B = surfactant concentration, and C = drug/lipid ratio (Table 1). The Box-Behnken design implemented using Design-Expert® software analysed the influence of varying surfactant concentration, lipid concentration, and drug/ lipid ratio on SLNs formation.

Polydispersity Index (PDI), mean Particle Size, and Zeta Potential Measurement

The PDI, mean particle size, and zeta potential of prednisolone-loaded SLNs formulations generated by Design-Expert software were determined by a Malvern Zetasizer Nano-ZS (Malvern Instruments, UK). Prior to measurement, each sample was diluted in a 1:10 ratio with distilled water in a beaker to minimise multiscattering effects. The diluted sample was transferred to a disposable zeta cuvette and placed in the instrument's sample holder.

Transmission Electron Microscopy (TEM)

The morphology of prednisolone-loaded SLNs was characterised using a JEM-2100Plus transmission electron microscope (JEOL, Tokyo, Japan) operating at an accelerating voltage of 200 kV. Before imaging, the samples were diluted with distilled water and sonicated for 3 min to deagglomerate the nanoparticles and disperse the base fluid [14]. A drop of the diluted sample was then deposited onto a polyvinyl formaldehyde resin (FORMVAR) carbon film copper grid and allowed to adsorb for 5 min. Next, the sample was stained with 2% (w/w) phosphotungstic acid for 1 min to enhance contrast. The excess staining solution was removed using filter paper, leaving a thin aqueous film containing SLNs on the grid surface. The prepared

sample was mounted onto a vacuum-controlled sample holder and imaged using an auto-fine coater.

Attenuated Total Reflectance-Fourier Transform Infrared Spectroscopy (ATR-FTIR)

Fourier transform infrared (FTIR) spectra of prednisolone-loaded SLNs were acquired using a Spectrum 100 spectrometer (Perkin Elmer, USA) equipped with a MIRacle ATR accessory (PIKE Technologies, Madison, USA). The sample was spread onto the zinc selenide crystal surface using a pressure clamp to maximise the sampling sensitivity and maintain close contact. Spectra were recorded with a resolution of 4 cm^{-1} and a scanning time of 1.5 min over a wavenumber range of 4000–660 cm^{-1}. Each sample was measured thrice, and the spectra were averaged.

RESULTS AND DISCUSSION

Data Analysis and Model Fitting

Design-Expert® software (Version 7.0) analysed the experimental data generated from the Box-Behnken design. This software facilitated the construction of the experimental design, generation of response surface plots, and investigation of independent factors influencing the responses. Table 1 summarises the 17 batches of prednisolone-loaded SLNs obtained using a modified emulsification-ultrasonication process with a three-level Box-Behnken design. The three independent factors, surfactant concentration, lipid concentration, and drug/lipid ratio, were chosen to optimise the nanoparticle characteristics.

The analysis of the experimental design using Design-Expert® revealed valuable insights and confirmed the importance of the statistical blueprint for successful experimentation. Notably, specific independent variables, including the drug/lipid ratio, Tween 20 concentration, and cetyl alcohol concentration, significantly influenced the obtained responses (particle size, PDI, and zeta potential). A quadratic model was determined to be appropriate, and an analysis of variance (ANOVA) was used to identify factors with significant effects on the responses. All 17 formulations generated by the software were analysed for their respective responses (zeta potential, PDI, and particle size).

Particle Size

The analysis of the Box-Behnken design for particle size revealed a quadratic model with a size range of 59.99 to 594.7 nm. The maximum-to-minimum ratio of 9.91332 is less than 10, indicating that no transformation is required. However, the ANOVA tests (Table 2) showed a non-significant model with an F-value of 1.22 and a P-value of 0.4060. Similarly, the "Lack of Fit F-value" of 1.55 suggested that there was no significant lack of fit as compared with pure error.

Table 1: Prednisolone-loaded SLNs prepared using a three-level Box-Behnken design.

Formulations/batches	Factors			Response		
	A: Cetyl alcohol (% w/w)	B: Tween 20 (% v/v)	C: Drug/ lipid ratio (% w/w)	Particle size (nm)	PDI	Zeta potential (mV)
1	7.50	5.00	0.00	424.07	0.99	-31.93
2	7.50	3.50	1.00	192.23	0.63	-28.60
3	7.50	3.50	1.00	400.27	0.53	-26.33
4	7.50	3.50	1.00	482.17	0.97	-30.90
5	5.00	3.50	2.00	545.70	0.88	-25.17
6	7.50	5.00	2.00	234.50	1.00	-20.67
7	5.00	2.00	1.00	85.40	1.00	-15.73
8	10.00	3.50	0.00	594.70	0.93	-25.57
9	10.00	5.00	1.00	335.97	0.92	-20.00
10	7.50	2.00	0.00	454.43	1.00	-23.60
11	7.50	3.50	1.00	220.87	0.90	-26.80
12	10.00	2.00	1.00	59.99	0.65	-22.50
13	10.00	3.50	2.00	374.30	0.64	-22.63
14	7.50	2.00	2.00	460.47	0.96	-34.27
15	7.50	3.50	1.00	419.90	1.00	-27.13
16	5.00	3.50	0.00	289.47	0.39	-32.37
17	5.00	5.00	1.00	296.87	0.47	-27.57

Although non-significant, the model equation highlighted the influence of independent factors on the particle size.

$$\text{Particle size} = +343.09 + 18.44\,A + 28.89\,B - 18.46\,C - 45.43\,A^2 - 103.10\,B^2 + 153.38\,C^2 + 16.13\,AB - 119.16\,AC - 48.90\,BC$$

Figure 1 presents response surface plots illustrating the combined effects of lipid concentration, drug/lipid ratio, and surfactant concentration on the particle size. Notably, none of the factors had a significant influence. Nevertheless, the positive coefficient estimates for lipid and surfactant concentrations suggest a trend of increasing particle size with their levels. Conversely, the drug/lipid ratio was negatively associated with particle size. Interestingly, the interaction terms revealed a positive effect for the lipid and surfactant combination, whereas the drug/lipid ratio interactions were negative.

This trend aligns with the existing literature. The increase in particle size with increasing lipid concentration was consistent with the reported coalescence tendencies at higher lipid levels [15]. Similarly, the positive influence of surfactant concentration has been attributed to the increased lipid/surfactant mass ratio, which promotes larger particles [16]. Conversely, higher drug/lipid ratios may enhance nanoemulsion viscosity owing to greater lipid content, potentially leading to larger particles [17].

Furthermore, insufficient surfactant concentrations at lower levels could contribute to incomplete particle surface coverage, increasing interfacial tension and promoting aggregation [18,19]. Consequently, higher surfactant concentrations and lower lipid levels typically favour smaller nanoparticles. However, it is crucial to acknowledge that several factors in the formulation process, including pH, sonication time, and temperature, can have a major impact on the size and stability of particles. This might potentially alter the observed trends [20–22].

Polydispersity Index (PDI)

The analysis of the Box-Behnken design for PDI identified a quadratic model as the best fit, with a range of 0.39 to 1.0 and a maximum-to-minimum ratio of 2.58. While ANOVA tests (Table 3) revealed a non-significant model (F-value = 2.26, P-value = 0.1349), the "Lack of Fit F-value" of 0.23 also implied an insignificant lack of fit.

Table 2. ANOVA for response surface reduced quadratic model of particle size.

ANOVA for Response Surface Quadratic Model							
Response: Particle size							
Source		*Sum of squares*	*DF*	*Mean Square*	*F Value*	*Prob > F*	
Model		2.244E+005	9	24934.34	1.22	0.4060	Not significant
	A	2720.27	1	2720.27	0.13	0.7261	
	B	6676.29	1	6676.29	0.33	0.5857	
	C	2726.91	1	2726.91	0.13	0.7258	
	A^2	8689.21	1	8689.21	0.42	0.5353	
	B^2	44758.71	1	44758.71	2.19	0.1826	
	C^2	99057.22	1	99057.22	4.84	0.0637	
	AB	1040.49	1	1040.49	0.051	0.8280	
	AC	56794.83	1	56794.83	2.78	0.1396	
	BC	9564.84	1	9564.84	0.47	0.5161	
Residual		1.432E+005	7	20453.91			
Lack of fit		76969.47	3	25656.49	1.55	0.3324	Not significant
Pure error		66207.92	4	16551.98			
Cor total		3.676E+005	16				

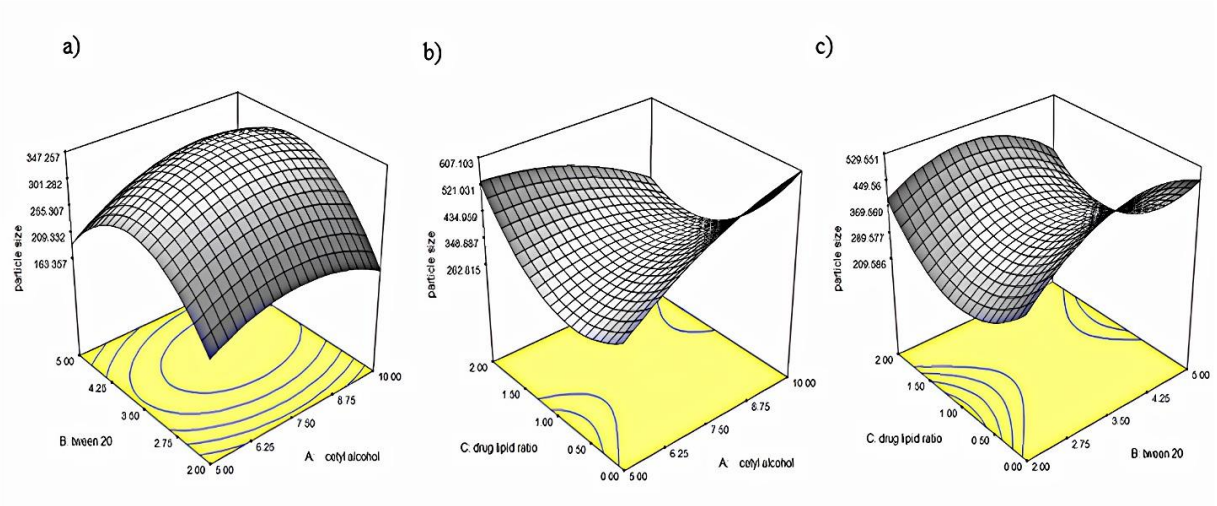

Figure 1. 3D response plots for the effects of a) lipid concentration and surfactant concentration, b) lipid concentration and drug/lipid ratio, and c) surfactant concentration and drug/lipid ratio on particle size.

PDI reflects the size distribution range within a lipidic nanocarrier system, where lower values (closer to 0) indicate greater uniformity, and higher values (approaching 1) represent broader diversity. The observed PDI value of 0.7 suggested a somewhat broad particle size distribution. In nanoparticle applications, PDIs below 0.7 generally signify enhanced stability [23].

The model equation presented the influence of independent factors on PDI, with positive coefficients indicating increasing trends and vice versa. Notably, statistical analysis of variance (Table 3) revealed significant effects of the interaction term involving both surfactant and lipid concentration (AB).

$$PDI = + 0.82 + 0.051\ A - 0.031\ B + 0.023\ C - 0.16\ A^2 + 0.12\ B^2 + 0.20\ AB - 0.19\ AC + 0.012\ BC$$

Table 3. ANOVA for the response surface reduced quadratic model of PDI.

ANOVA for Response Surface Quadratic Model							
Response: PDI							
Source		*Sum of squares*	*DF*	*Mean Square*	*F Value*	*Prob > F*	
Model		0.50	8	0.063	2.26	0.1349	Not significant
	A	0.021	1	0.021	0.75	0.4131	
	B	7.917E-003	1	7.917E-003	0.29	0.6077	
	C	4.247E-003	1	4.247E-003	0.15	0.7058	
	A^2	0.11	1	0.11	3.87	0.0846	
	B^2	0.059	1	0.059	2.13	0.1821	
	AB	0.16	1	0.16	5.71	0.0439	
	AC	0.15	1	0.15	5.46	0.0477	
	BC	6.334E-004	1	6.334E-004	0.023	0.8836	
Residual		0.22	8	0.028			
Lack of fit		0.041	4	0.010	0.23	0.9111	Not significant
Pure error		0.18	4	0.045			
Cor total		0.72	16				

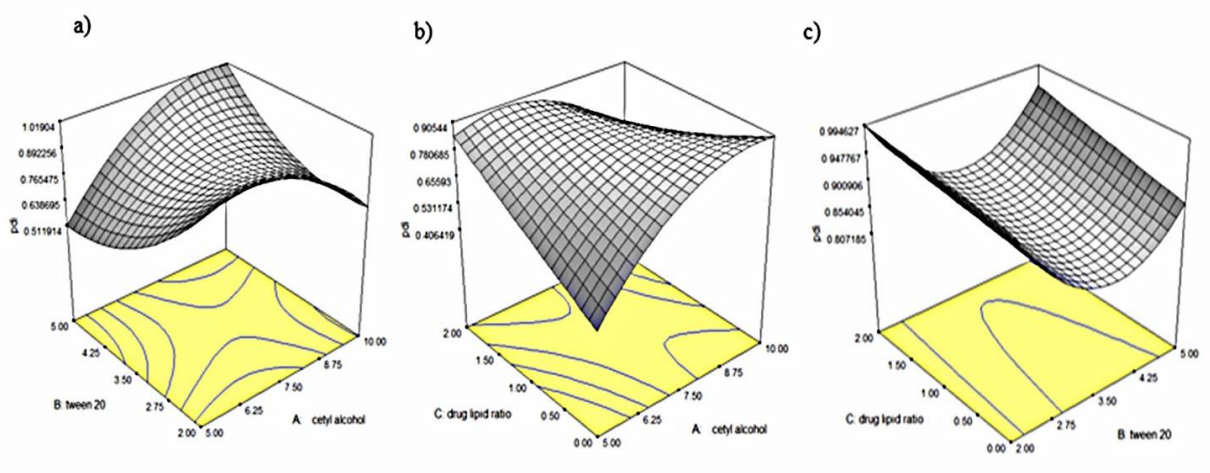

Figure 2. 3D response plots for the effects of a) lipid concentration and surfactant concentration, b) lipid concentration and drug/lipid ratio, and c) surfactant concentration and drug/lipid ratio on PDI.

As depicted in Figure 2, the combined influence of surfactant and lipid concentrations on PDI was visualised through response surface plots. The significant interaction AB demonstrated a positive effect, implying that increasing both factors led to a broader PDI. This aligns with reports suggesting a link between a higher lipid content and larger particle size distributions [19, 24]. Additionally, surfactants can initially increase steric resistance and particle stability through surface adsorption [25, 26]. However, exceeding optimal surfactant levels can potentially destabilise the system owing to excess surfactant accumulation and bridging effects, leading to aggregation and broader size distributions [26]. This rationale explains the observed increase in PDI with a joint increase in surfactant and lipid concentrations.

Zeta Potential

The analysis of the Box-Behnken design for zeta potential revealed a significant quadratic model (F-value = 21.31, P-value = 0.0003) ranging from -34.37 to -15.73 mV (Table 4). Although the drug/lipid ratio and surfactant concentration individually lacked significant effects ($P > 0.05$), lipid concentration was identified as a significant factor influencing zeta potential (Table 4). Notably, terms A, A^2, B^2, C^2, AB, and BC within the model equation contributed significantly. The "Lack of Fit F-value" of 0.29 suggested an insignificant lack of fit compared to the pure error.

Zeta potential, which reflects the charge acquired by particles in a medium, serves as a crucial criterion for colloidal system stability. Larger absolute values (positive or negative) indicate stronger interparticle repulsion, reduced aggregation, and enhanced stability [27]. The polynomial model equation depicted the influence of independent factors on the zeta potential, with positive coefficients indicating increasing trends and vice versa. ANOVA further revealed a significant interaction between lipid and surfactant concentrations on the zeta potential (Figure 3). Although all components, including the drug/lipid ratio, showed positive coefficient estimates, not all of them were statistically significant.

$$\text{Zeta potential} = -29.08 + 3.61\,A + 0.91\,B + 0.41\,C + 4.89\,A^2 + 5.57\,B^2 - 4.11\,C^2 + 6.42\,AB + 0.79\,AC + 5.48\,BC$$

Notably, the zeta potential decreased negatively with increasing surfactant concentration. The negatively charged surface potential of the lipidic particles suggested long-term stability through electrostatic repulsion between the particles [28]. Moreover, using a nonionic surfactant contributed to steric stabilisation, further preventing aggregation in the colloidal system [29]. In general, the influence of chemical properties, including the concentrations of lipids and surfactants, on zeta potential values has significant effects on the colloidal stability of the formulation.

Table 4. ANOVA for response surface reduced quadratic model of zeta potential.

ANOVA for Response Surface Quadratic Model							
Response: Zeta potential							
Source		*Sum of squares*	*DF*	*Mean Square*	*F Value*	*Prob > F*	
Model		696.65	9	77.41	21.31	0.0003	Significant
	A	104.40	1	104.40	28.74	0.0011	
	B	6.60	1	6.60	1.82	0.2197	
	C	1.36	1	1.36	0.37	0.5598	
	A^2	100.85	1	100.85	27.76	0.0012	
	B^2	130.59	1	130.59	35.94	0.0005	
	C^2	70.98	1	70.98	19.54	0.0031	
	AB	164.69	1	164.69	45.33	0.0003	
	AC	2.51	1	2.51	0.69	0.4336	
	BC	120.27	1	120.27	33.10	0.0007	
Residual		25.43	7	3.63			
Lack of fit		4.57	3	1.52	0.29	0.8302	Not significant
Pure error		20.86	4	5.22			
Cor total		722.08	16				

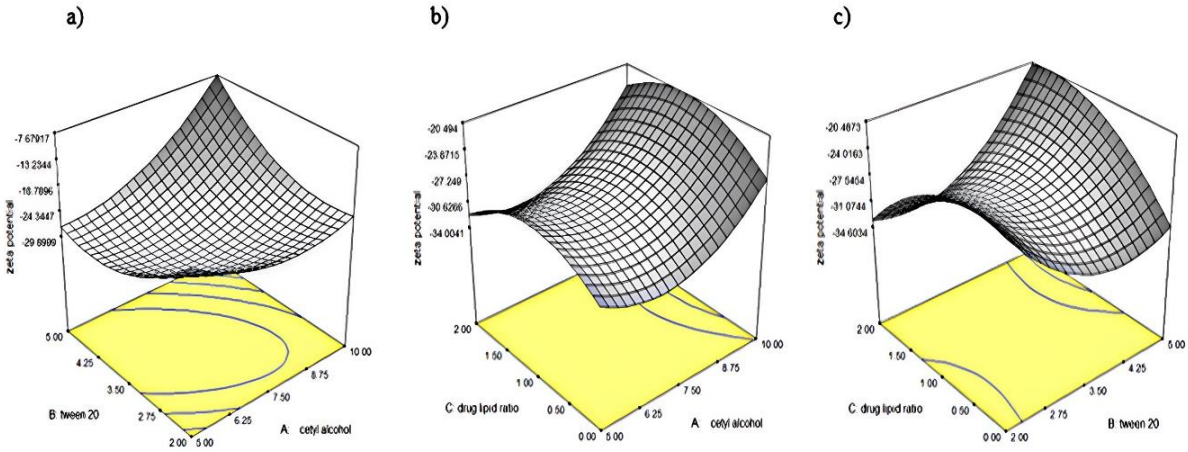

Figure 3. 3D response plots for the effects of a) lipid concentration and surfactant concentration, b) lipid concentration and drug/lipid ratio, and c) surfactant concentration and drug/lipid ratio on zeta potential.

Transmission Electron Microscopy (TEM)

TEM analysis determined the morphology and size distribution of prednisolone-loaded SLNs. The obtained photomicrographs displayed nanoparticles with predominantly nano-cuboidal and nano-rod shapes, exhibiting smooth surfaces and minimal aggregation. The particle sizes observed in the micrographs were consistent with those measured by the Malvern particle size analyser, remaining below 500 nm.

Figure 4. TEM photomicrograph of the selected formulation (lipid: 7.5% (w/w), surfactant: 3.5% (v/v) drug/lipid ratio: 1% (w/w)) of prednisolone-loaded SLNs at 11,500x magnification.

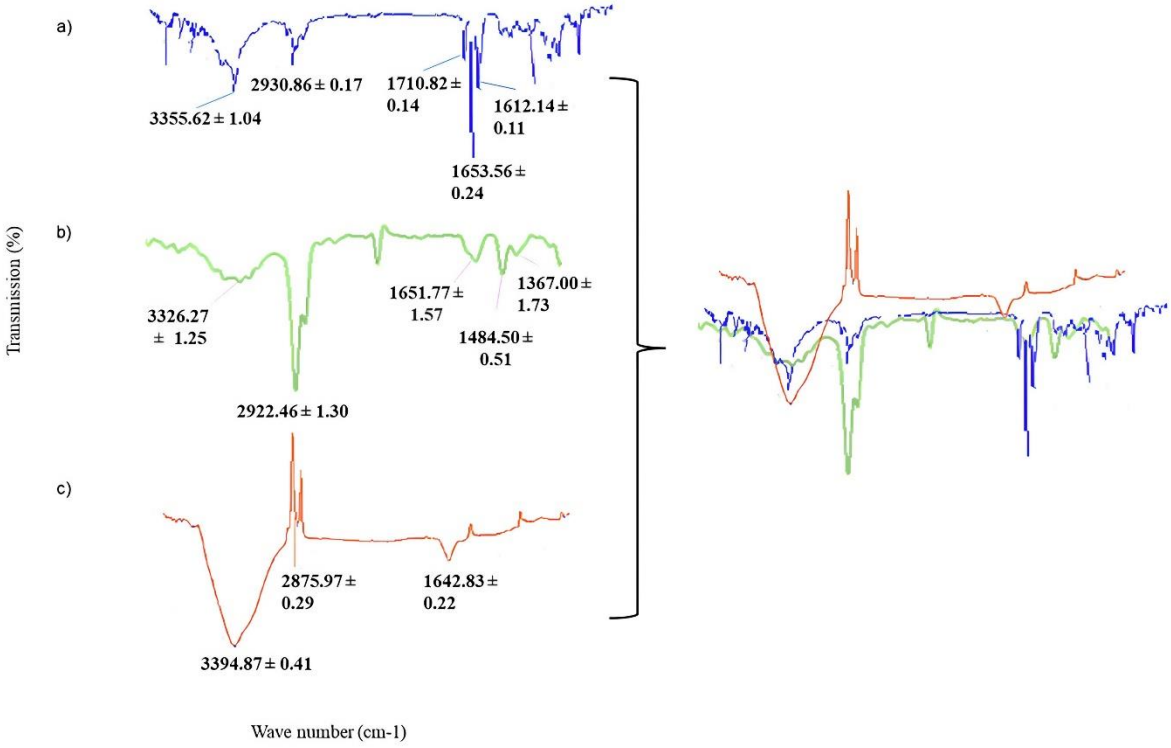

Figure 5. ATR-FTIR spectra of a) prednisolone, b) cetyl alcohol, and c) prednisolone-loaded SLNs (lipid concentration: 7.5% (w/w), surfactant concentration: 3.5% (v/v), drug/lipid ratio: 1% (w/w)).

ATR-FTIR

ATR-FTIR spectroscopy investigated the chemical composition of prednisolone, cetyl alcohol, and prednisolone-loaded SLNs (Figure 5). This technique facilitated the identification and confirmation of characteristic functional groups, aiding the detection of cetyl alcohol and prednisolone within nanoparticle formulations [30].

Prednisolone displayed well-defined characteristic peaks associated with a broad hydrogen-bonded

hydroxyl stretch (3355 ± 1.04 cm^{-1}), strong methylene C-H stretch (2930 ± 0.17 cm^{-1}), intense C=O stretching (1710 ± 0.14 cm^{-1}), alkenyl C=C stretch (1653 ± 0.24 cm^{-1}), and open chain azo N=N bond (1612.14 ± 0.11 cm^{-1}) (Figure 5a). Cetyl alcohol exhibited characteristic peaks corresponding to a broad hydrogen-bonded hydroxyl stretch, a methyl C-H stretch, an alkenyl C=C stretch, and methyl C-H bending at 3326 ± 1.25, 2922 ± 1.30, 1651 ± 1.57, and 1367 ± 1.73 cm^{-1}, respectively (Figure 5b).

Interestingly, drug absorption peaks in the 1600-3400 cm^{-1} region were partially obscured upon incorporation of prednisolone into the SLNs. However, three distinct prednisolone peaks initially identified at 1653 ± 0.24, 2930 ± 0.17, and 3355 ± 1.04 cm^{-1} were still observed at corresponding positions in the prednisolone-loaded SLNs spectrum at 1642 ± 0.22, 2875 ± 0.29, and 3394 ± 0.42 cm^{-1} (Figure 5a and c). Analysis of the combined spectra revealed that the putative absorption peaks of cetyl alcohol at 3394 ± 0.41, 2875 ± 0.29, and 1642 ± 0.22 cm^{-1} in the prednisolone-loaded SLNs spectrum overlapped with those of prednisolone (Figure 5b and c). These findings suggested the successful incorporation of prednisolone into the solid lipid matrix of nanoparticles.

CONCLUSION

Although the developed prednisolone-loaded SLNs demonstrated promising qualities, they offer the potential for further refinement. The particle size and uniformity could benefit from fine-tuning the lipid and surfactant concentrations within the desired range. Similarly, optimising these factors alongside others, such as pH, temperature, and sonication time, might improve the broad size distribution indicated by PDI. The favourable zeta potential, influenced significantly by lipid concentration, suggests good electrostatic repulsion and stability; however, further exploration may unlock additional stability enhancements. TEM analysis confirmed successful nanoparticle formation with smooth morphology and minimal aggregation. Notably, ATR-FTIR analysis revealed drug incorporation; however, partial peak masking highlights the need for further optimisation to ensure consistent drug loading. In conclusion, the Box-Behnken design has yielded promising progress. However, further investigation into independent factors and their interactions is recommended to achieve truly optimal prednisolone-loaded SLNs for effective drug delivery.

ACKNOWLEDGEMENTS

This research was funded by the Ministry of Higher Education Malaysia under the Fundamental Research Grants Scheme (FRGS/1/2023/STG05/UITM/02/5). We are also grateful to the Universiti Teknologi MARA, Malaysia, for providing crucial facility support.

REFERENCES

1. Alahmadi, F., Peel, A., Keevil, B., Niven, R. and Fowler, S. J. (2021) Assessment of adherence to corticosteroids in asthma by drug monitoring or fractional exhaled nitric oxide: A literature review. *Clinical & Experimental Allergy*, **51(1)**, 49–62.

2. Brown, K. K., Rehmus, W. E. and Kimball, A. B. (2006) Determining the relative importance of patient motivations for nonadherence to topical corticosteroid therapy in psoriasis. *Journal of American Academy of Dermatology*, **55(4)**, 607–613.

3. Stewart, S. F., Moon, Z. and Horne, R. (2023) Medication nonadherence: Health impact, prevalence, correlates and interventions. *Psychology & Health*, **38(6)**, 726–765.

4. Ghasemiyeh, P. and Mohammadi-Samani, S. (2020) Potential of nanoparticles as permeation enhancers and targeted delivery options for skin: Advantages and disadvantages. *Drug Design Development and Therapy*, **14**, 3271–3289.

5. Yu, Y. Q., Yang, X., Wu, X. F., Fan, Y. B. (2021) Enhancing permeation of drug molecules across the skin via delivery in nanocarriers: Novel strategies for effective transdermal applications. *Frontiers in Bioengineering and Biotechnology*, **9**, 646554.

6. Fan, W., Peng, H., Yu, Z., Wang, L., He, H., Ma, Y., Qi, J., Lu, Y. and Wu, W. (2022) The long-circulating effect of pegylated nanoparticles revisited via simultaneous monitoring of both the drug payloads and nanocarriers. *Acta Pharmaceutica Sinica B.*, **12(5)**, 2479–2493.

7. Haroon, H. B., Hunter, A. C., Farhangrazi, Z. S. and Moghimi, S. M. (2022) A brief history of long circulating nanoparticles. *Advance Drug Delivery Reviews*, **188**, 114396.

8. Ezzati Nazhad Dolatabadi, J, Hamishehkar, H., Eskandani, M. and Valizadeh, H. (2014) Formulation, characterization and cytotoxicity studies of alendronate sodium-loaded solid lipid nanoparticles. *Colloids and Surfaces B. Biointerfaces*, **117**, 21–28.

9. Hao, J., Fang, X., Zhou, Y., Wang, J., Guo, F., Li, F. and Peng, X. (2011) Development and optimization of solid lipid nanoparticle formulation for ophthalmic delivery of chloramphenicol using a Box-Behnken design. *International Journal of Nanomedicine*, **6**, 683–692.

10. Bakhaidar, R. B., Naveen, N. R., Basim, P., Murshid, S. S., Kurakula, M., Alamoudi, A. J., Bukhary,

D. M., Jali, A. M., Majrashi, M. A., Alshehri, S., Alissa, M. and Ahmed, R. A. (2022) Response Surface Methodology (RSM) powered formulation development, optimization and evaluation of thiolated based mucoadhesive nanocrystals for local delivery of simvastatin. *Polymers (Basel)*, **14(23)**, 5184.

11. Lamidi, S., Olaleye, N., Bankole, Y., Obalola, A., Aribike, E. and Adigun, I. (2023) Applications of Response Surface Methodology (RSM) in Product Design, Development, and Process Optimization. In: Response Surface Methodology - Research Advances and Applications. *IntechOpen Limited, United Kingdom*.

12. Zur Mühlen, A., Schwarz, C. and Mehnert, W. (1998) Solid lipid nanoparticles (SLN) for controlled drug delivery–drug release and release mechanism. *European Journal of Pharmaceutics and Biopharmaceutics*, **45(2)**, 149–155.

13. Pradhan, M., Singh, D. and Singh, M, R. (2017) Fabrication, optimization and characterization of triamcinolone acetonide loaded nanostructured lipid carriers for topical treatment of psoriasis: Application of Box Behnken design, in vitro and ex vivo studies. *Journal of Drug Delivery Science and Technology*, **41**, 325–333.

14. Shah, T. R., Koten, H. and Ali, H. M. (2020) Performance effecting parameters of hybrid nanofluids. In: Hybrid Nanofluids for Convection Heat Transfer. *Academic Press, United States*.

15. Emami, J., Mohiti, H., Hamishehkar, H. and Varshosaz, J. (2015) Formulation and optimization of solid lipid nanoparticle formulation for pulmonary delivery of budesonide using Taguchi and Box-Behnken design. *Research Pharmaceutical Sciences*, **10(1)**, 17–33.

16. Sarmento, B., Ferreira, D., Veiga, F. and Ribeiro, A. (2006) Characterization of insulin-loaded alginate nanoparticles produced by ionotropic pre-gelation through DSC and FTIR studies. *Carbohydrate Polymers*, **66(1)**, 1–7.

17. Vitorino, C., Carvalho, F. A., Almeida, A. J., Sousa, J. J. and Pais, A. A. (2011) The size of solid lipid nanoparticles: An interpretation from experimental design. *Colloids and Surfaces B. Biointerfaces*, **84(1)**, 117–130.

18. Kumar, S., Narayan, R., Ahammed, V., Nayak, Y., Naha, A. and Nayak, U. Y. (2018) Development of ritonavir solid lipid nanoparticles by Box Behnken design for intestinal lymphatic targeting. *Journal of Drug Delivery Science and Technology*, **44**, 181–189.

19. Badawi, N., El-Say, K., Attia, D., El-Nabarawi, M., Elmazar, M. and Teaima, M. (2020) Development of pomegranate extract-loaded solid lipid nano-particles: Quality by design approach to screen the variables affecting the quality attributes and characterization. *ACS Omega*, **5(34)**, 21712–21721.

20. Marciniak, L., Nowak, M., Trojanowska, A., Tylkowski, B. and Jastrzab, R. (2020) The effect of pH on the size of silver nanoparticles obtained in the reduction reaction with citric and malic acids. *Materials (Basel)*, **13(23)**, 5444.

21. Pradhan, S., Hedberg, J., Blomberg, E., Wold, S. and Wallinder, I. O. (2016) Effect of sonication on particle dispersion, administered dose and metal release of non-functionalized, non-inert metal nanoparticles. *Journal of Nanoparticle Research*, **18**, 285.

22. Jiang, X. C., Chen, W. M., Chen, C. Y., Xiong, S. X. and Yu, A. B. (2011) Role of temperature in the growth of silver nanoparticles through a synergetic reduction approach. *Nanoscale Research Letters*, **6**, 32.

23. Danaei, M., Dehghankhold, M., Ataei, S., Hasanzadeh, D. F., Javanmard, R., Dokhani, A., Khorasani, S. and Mozafari, M. R. (2018) Impact of particle size and polydispersity index on the clinical applications of lipidic nanocarrier systems. *Pharmaceutics*, **10(2)**, 57.

24. Tiyaboonchai, W., Tungpradit, W. and Plianbangchang, P. (2007) Formulation and characterization of curcuminoids loaded solid lipid nanoparticles. *International Journal of Pharmaceutics*, **337(1–2)**, 299–306.

25. Gonzalez, F. G., Vilchez, M. A. C. and Hidalgo-Alvarez, R. (1991) Adsorption of anionic surfactants on positively charged polystyrene particles II. *Colloidal and Polymer Science*, **269**, 406–411.

26. Wang, C., Cui, B., Guo, L., Wang, A., Zhao, X., Wang, Y., Sun, C., Zeng, Z., Zhi, H., Chen, H., Liu, G. and Cui, H. (2019) Fabrication and evaluation of lambda-cyhalothrin nanosuspension by one-step melt emulsification technique. *Nanomaterials (Basel)*, **9(2)**, 145.

27. Levy, M. Y., Schutze, W., Fuhrer, C. and Benita, S. (1994) Characterization of diazepam submicron emulsion interface: Role of oleic acid. *Journal of Microencapsulation*, **11(1)**, 79–92.

28. Gupta, M. and Vyas, S. P. (2012) Development, characterization and in vivo assessment of effective lipidic nanoparticles for dermal delivery of

fluconazole against cutaneous candidiasis. *Chemistry and Physics of Lipids*, **165(4)**, 454–461.

29. Anselmo, A. C. and Mitragotri, S. (2014) Cell-mediated delivery of nanoparticles: Taking advantage of circulatory cells to target nanoparticles. *Journal of Controlled Release*, **190**, 531–541.

30. Shahraeini, S. S., Akbari, J., Saeedi, M., Morteza-Semnani, K., Abootorabi, S., Dehghanpoor, M., Rostamkalaei, S. S. and Nokhodchi, A. (2020) Atorvastatin solid lipid nanoparticles as a promising approach for dermal delivery and an anti-inflammatory agent. *AAPS PharmSciTech*, **21(7)**, 263.